

Formulation of bortezomib human serum albumin nanoparticles, *in vitro* and *in vivo* evaluation

Areej W. ALHAGIESA^{1*}, Mowafaq M. GHAREEB²

¹ University of Kufa, College of Pharmacy, Department of Pharmaceutics, Najaf, Iraq

² University of Baghdad, College of Pharmacy, Department of Pharmaceutics, Baghdad, Iraq

ABSTRACT

Bortezomib (BTZ) is a selective proteasome inhibitor whose anticancer activity results from disrupting regulated protein turnover, leading to apoptosis. It is highly potent but lacks specificity and shows limited activity against solid tumors. This project aims to formulate BTZ as Human Serum Albumin Nanoparticles (HSA NPs) to improve its sensitivity and selectivity towards solid tumors. These albumin nanoparticles enable both passive and active targeting. Passive targeting occurs through the enhanced permeation and retention (EPR) effect of nanoparticles, while the overexpression of albumin receptors on tumor cells facilitates active targeting. BTZ HSA NPs have been prepared using the desolvation method. *In vitro* characterisation involved particle size (PS), polydispersity index (PDI), entrapment efficiency (EE%), particle morphology, and an *in vitro* release study. The optimised formula was then evaluated for its anti-tumor activity *in vivo* using BALB/c mice, where the tumor volume was measured, and a histopathological analysis of the tumor tissue was performed. The optimised formula has PS, PDI, and EE% of (28) nm, 0.045, and 36%, respectively. The particles exhibit an almost spherical morphology and a controlled-release profile, with approximately 85% of BTZ released within 24 hours. On the other hand, *in vivo*, the NPs showed a significant decrease in tumor volume compared with the group that received only pure

* Corresponding author: Areej W. ALHAGIESA

E-mail: areej.w.alhagiesaa@uokufa.edu.iq

ORCID:

Areej W. ALHAGIESA: 0009-0006-2675-8364

Mowafaq M. GHAREEB: 0000-0002-9968-7396

(Received 2 Dec 2026, Accepted 21 Jan 2026)

BTZ or phosphate-buffered saline (PBS). The histopathological study showed better tumor aggressiveness (lower mitotic count and nuclear pleomorphism), increased apoptosis, and improved immune cell infiltration. Formulation of BTZ as HSA NPs is a successful approach to enhance its activity and selectivity against cancer cells. The desolvation method is a reliable, reproducible method for obtaining these NPs.

Keywords: Bortezomib, human serum albumin nanoparticles, anticancer targeting, proteasome inhibitors, tumor targeting

INTRODUCTION

Bortezomib (BTZ) is the first-in-class selective proteasome inhibitor. Firstly, it was approved for the treatment of multiple myeloma and mantle cell lymphoma. It acts by disrupting regulated protein turnover, leading to the accumulation of misfolded proteins and the induction of apoptosis in tumor cells^{1,2}. Several studies have investigated the use of BTZ for the treatment of solid tumors. BTZ has some biological and pharmaceutical constraints such as limited aqueous solubility, high incidence of toxicity and adverse effects such as thrombocytopenia and peripheral neuropathy, suboptimal tumor selectivity, and the emergence of resistance by malignant cells³. Reported resistance mechanisms include alterations in the $\beta 5$ proteasome subunit, adaptive upregulation of proteasome activity, enhanced stress-response pathways, and drug efflux, all of which can diminish the therapeutic response in solid tumor settings^{4,5}.

Many researchers have been developing formulations to enhance BTZ activity and improve selectivity. Nanoparticles have been widely used to improve the pharmacokinetic and pharmacodynamic profile of BTZ in solid tumors. These include liposomes, polymeric micelles, dendrimers, nanogels, and inorganic NPs, to enhance solubility, prolong circulation time, and improve targeting and drug concentration at tumor sites. Nanocarriers provide passive targeting through the enhanced permeation and retention effect (EPR), which is attributed to the leaky nature of tumor cells and limited lymphatic drainage. However, EPR is present in most tumor types, which motivates researchers to develop formulations that combine passive targeting with nanomaterials and active targeting, which usually utilises receptor-mediated targeting to improve intratumoral accumulation and cellular uptake⁶⁻⁹.

Human serum albumin (HSA) is a promising system for BTZ delivery. As albumin is biocompatible and biodegradable, non-immunogenic, possesses

a long circulatory half-life, and interacts with endothelia and tumor microenvironments, it represents an ideal candidate for drug delivery. In addition to passive EPR-mediated accumulation, albumin could also target active transport and/or retention machinery associated with cancer. Endothelial cell gp60 (albondin) initiates caveolae-mediated albumin transcytosis across the vascular wall, and the matricellular protein SPARC (secreted protein acidic and rich in cysteine), which is frequently overexpressed by tumors and in stromal tissue, binds albumin from within the interstitium and can promote local retention. Taken together, these features provide a biologically based pathway to preferentially enrich albumin-based nanomedicines in tumors compared with normal tissues, beyond passive accumulation, potentially enhancing the therapeutic index. Albumin interaction and possible elongation of the systemic half-life by the neonatal Fc receptor (FcRn; salvage/recycling) may also aid drug delivery to target tissues¹⁰⁻¹³.

The desolvation technique is a widely used, scalable process for preparing albumin nanoparticles, followed by particle stabilisation through covalent crosslinking. Two of the most common crosslinking agents include (i) glutaraldehyde (Glut), which leads to Schiff-base linkages with lysine, reducing mechanical stability, and (ii) carbodiimide chemistry (EDC/NHS), facilitating amide bond formation between carboxyl and amine without adding an external linker. The choice and optimisation of the crosslinker determine the particle size distribution, drug entrapment, and release kinetics, which, in turn, influence *in vivo* behavior^{14,15}.

In the present study, we aimed to generate BTZ HSA nanoparticles by the desolvation method, crosslinked with Glut or EDC, with the intention of 'dual targeting': passive tumor accumulation (EPR) and active enrichment through albumin-gp60 transcytosis / SPARC-associated retention as reported in the literature. The prepared nanoparticles were fully characterised regarding their physicochemical features (size, polydispersity index, and morphology), drug encapsulation, *in vitro* drug release, and *in vitro* cytotoxicity study using the 4T1 cell line. In addition, a physical stability assessment has been conducted for the prepared NPs for 60 days.

Finally, we conducted an *in vivo* biological investigation regarding antitumor efficacy by measuring tumor volume and histopathological evaluation of tumor tissues after treatment. This study aims to verify the speculation that albumin-based nanoformulation can facilitate BTZ transport into solid tumors and reduce systemic toxicity.

METHODOLOGY

Materials

HSA, BTZ, and Glut were obtained from Xian International Company, China. HPLC-grade water and methanol, phosphate buffer salts, and acetone were purchased from Himedia Company, India. EDC was purchased from Macklin Company in China.

Method of HPLC

Optimisation of the HPLC method was performed on the Knauer HPLC device in Germany. In which the method was optimised and validated for the detection and quantification of BTZ in the prepared formulation. Using Nova Atom C18 column, 4.6mm × 250 mm, 5µm, 120°A, and Nova Z-Guard C18core 4.6 mm × 10mm, 5µm, 120°A. The mobile phase was a mixture of methanol and water (70:30%), with a flow rate of 1 mL/min. Detection was performed with a UV detector at 270 nm.

Formulation of BTZ HSA NPs

BTZ HSA NPs were prepared by the desolvation (precipitation) method in which 200 mg of HSA were dissolved in 5 ml DW and 15 mg of BTZ were dissolved in different volumes of different antisolvents as represented by Table 1. The organic solvent (antisolvent for the albumin solution) is added dropwise to the albumin solution using a syringe pump at a rate of 1 ml/min until turbidity appears, indicating the formation of ANP. The formulated NPs were then stabilised by the addition of an equimolar amount of different crosslinkers to the amount of BSA used in each formula. Each formula was left on a magnetic stirrer for 24 hours, after which the formed NPs were separated from free BTZ and excess crosslinker by centrifugation at 15,000 rpm for 25 minutes. The precipitated HSA NPs were then redispersed in DW to return to the original volume of 5 ml for further analysis^{16,17}.

Characterization of the BTZ HSA NPs

Measuring PS and PDI

The redispersed NPs were analysed by ABT9000 nanoparticle size analyser to measure PS and PDI. The measurement was done at a constant temperature of 25°C and a scattering angle of 90°. This device also measures PDI, which indicates the particle size distribution of the prepared nanoparticles within the formulation. Low-level PDI indicates a monodispersed formulation (PDI 0-0.05), while higher PDI values indicate a polydisperse formulation (PDI > 0.7)^{18,19}.

Determination of entrapment efficiency

EE% of the prepared NP was determined by the indirect method. The supernatant collected after centrifugation of the prepared NP was analyzed by HPLC to determine the BTZ concentration. Then, the amount of BTZ encapsulated within the NP was calculated using the equation below^{20,21}.

$$EE = \frac{\text{total amount of BTZ} - \text{amount of BTZ encapsulated within the NP}}{\text{total amount of BTZ}} * 100\% \text{ [Eq 1]}$$

In vitro release of BTZ HSA NPs

The release study of BTZ from the prepared nanoparticles was carried out using a digital magnetic stirrer (Jonalab Company, China) set at 37°C and 100 rpm. A 100 mL volume of release medium was placed in a 200 mL beaker, which was positioned inside a water bath. The release medium consisted of acetate buffer (pH 5.5 and pH 7.4), simulating the tumor microenvironment and systemic circulation, to which either BTZ nanoparticles or pure BTZ was added. Two milliliters of the dissolution medium were withdrawn at different time intervals (1, 2, 4, 6, 8, 12, and 24 hours). Each sample was centrifuged for 15 min at 6000 rpm. The supernatant is filtered using a syringe filter 0.22 µm and allowed to run by the HPLC to determine the concentration of the dissolved BTZ in each sample. 2 ml of the fresh media is added to the precipitated NP, mixed well, and then returned to the dissolution media to maintain the volume (100 ml of the dissolution media). The concentration of BTZ was determined by converting the HPLC absorbance to the validated calibration curve²².

Morphology of BTZ HSA NPs

A few drops of the suspension containing BTZ HSA NPs were placed on 300 mesh copper grids, negatively stained with 2% uranyl acetate, air-dried, and imaged at 100 kV. The samples were then analysed by TEM to obtain morphological characterization^{23,24}.

Hemolysis test

Eight samples of BTZ HSA NPs with varying concentrations, as shown in Table 2, were allowed to be incubated with human erythrocytes in PBS for 30 min at 37°C^{25,26}. The samples were then centrifuged, and the supernatant was examined at 540 nm to measure absorbance. Subsequently, the hemolysis was measured according to the following equation:

$$H\% = \frac{A_{\text{sample}} - A_{\text{negative control}}}{A_{\text{positive control}} - A_{\text{negative control}}} * 100\% \quad [\text{Eq 2}]$$

Where, A_{sample} is the absorbance of the sample (BTZ HSA NPs) in PBS, $A_{\text{positive control}}$ is the absorbance of Erythrocyte with distilled water and $A_{\text{negative control}}$ is the absorbance of Erythrocyte in phosphate buffer.

***In vitro* cytotoxicity study**

This study is performed using the MTT (3-[4,5-dimethyl- thiazol-2-yl]-2,5-diphenyltetrazoliumbromide) cell viability assay. 4T1 cells were seeded in 96-well plates for up to 48 h under standard incubation conditions of a humidified atmosphere at 37°C, 5% CO₂, and Dulbecco's Modified Eagle Medium (DMEM) in a laminar flow hood under aseptic conditions. The cells were treated with three different preparations: blank ANP, BTZ solution, and BTZ HSA NPs at various concentrations (0.5, 1, 2.5, 5, 10, 25, 50 ng/ml) for the drug and drug-incorporated NPs, and (10, 20, 50, 250, 500, 1000 ng/ml) for the blank NPs. After 48 h, the DMEM was replaced with fresh medium containing 10% MTT (0.5 mg/mL), and the plates were incubated for an additional 48 h for the cytotoxicity study. Then 100 µL DMSO was added to each well to replace the culture medium and dissolve the insoluble formazan crystals²⁷. The absorbance of each well was measured using an Asys High-tech Eliza reader spectrophotometer at 570 nm, and cell viability was calculated using the equation below:

$$\text{Cell viability \%} = \frac{A \text{ of treated cells}}{A \text{ of controll cells}} * 100\% \quad [\text{Eq 3}]$$

Antitumor activity

Eighteen female Balb/c mice were chosen to have the 4T1 cells injected into them. After two weeks, the tumors have developed. The mice were divided into three groups (n=6 for each group). The first group received BTZ HSA NPs, the second group received a pure BTZ solution, and the third group received only PBS. The treatment was administered three times weekly for 2 weeks, and tumor size was measured using a vernier caliper to assess antitumor activity^{28,29}. Tumor volume is measured based on the following equation:

$$\text{Tumor volume} = \frac{\text{length} * (\text{width})^2}{2} \quad [\text{Eq 4}]$$

Histopathology

After completing the 14-day treatment, mice were sacrificed, and histopathological assessment was performed on the tumor tissues of the three groups: Control, which received PBS; BTZ, which received pure BTZ solution; and BTZ HSA NPs, which received the prepared NPs. First, the tissues were fixed in 10% neutral buffered formalin; then, the tissue slices were embedded in paraffin, and the sections were deparaffinized. Samples were stained with hematoxylin and eosin. Images of the slides were captured under a microscope (Nikon ECLIPSE, 40× and 100× magnification) for histopathological examination³⁰.

Stability study

The stability study was performed on the final BTZ HSA NPs in liquid form at 4 and 25°C for 2 months. Each formula was examined for PS, PDI, and EE% every 2 weeks^{31,32}.

Statistical analysis

The results of this project are presented as average \pm SD, n=3. All the statistical analyses were performed with SPSS version 26.0 (SPSS Inc., Chicago, IL, USA). One-way ANOVA was used to compare means, and a p-value less than 0.05 was considered significant³³. The data were normally distributed and followed by Tukey's post-hoc test for pairwise comparisons^{34,35}.

RESULTS and DISCUSSION

Particle size, polydispersity index, and entrapment efficiency

The PS of the prepared formulas ranged from (24-1675) nm, as shown in Table 1. This table also indicates the PDI and EE% of the prepared NPs. Different variables have been utilised: volume and type of the antisolvent, two different crosslinkers (EDC and Glut), and stirrer speed.

Table 1. The formulation components and the variables affecting the formulation

Formula Name	Antisolvent Name	Antisolvent Volume (ml)	Crosslinker Type	Stirrer Speed (rpm)	PS	PDI	EE%
F31	Acetone	3.8	EDC	600	28.8 ± 6.08	0.045 ± 0.028	36.16 ± 1.75
F32	Acetone	4.5	EDC	600	143.26 ± 21.5	0.258 ± 0.083	34.43 ± 1.40
F33	Acetone	3.8	Glut	600	688.43 ± 37.5	0.010 ± 0.003	35.49 ± 3.6
F34	Ethanol	4.5	EDC	600	1672.34 ± 29.09	0.046 ± 0.02	25.93 ± 1.97
F35	Acetone	3.8	EDC	1000	78.67 ± 11.01	0.229 ± 0.065	7.67 ± 2.51

Two antisolvents have been used as desolvating agents for albumin solutions, namely acetone and ethanol. Acetone exhibited a lower PS distribution and the smallest PS, with the least volume, as shown in Figure 1. So, the formula with the 3.8 ml acetone as a desolvating agent has a PS (28.8 ± 6.08) nm. This result aligns with the findings of Mohammad-Beigiet et al. (2016), who also reported that acetone exhibited the smallest PS and the lowest antisolvent volume³⁶.

The PS of ANP increases with speed. This may be due to increased motion and turbulence, leading to agglomeration and growth of the NPs, as observed by Elham Sadat Taheri; however, this is in contrast to B. von Storp's results, which show that PS decreases as speed increases. However, it reaches an optimum speed close to that in this project³⁷⁻³⁹.

Two crosslinkers were used: Glut and EDC. The NPs stabilised by EDC showed a smaller PS distribution compared with the NPs stabilised by Glut. These results align with the results obtained by Garcia-Garrido⁴⁰. The effect of process variables on PS is illustrated in Figure 1.

The PDI of the resultant formula ranged from 0.01 to 0.2, which is typically indicative of monodispersity. It indicates a narrow size distribution, a sign of stable nanoformulation and a limited risk of particle growth⁴¹.

The EE% of the resultant formulas is comparable, and they were almost the same, as shown in Figure 2. The EE% for the formulas F31, F32, and F33 was about 35%. In contrast, for the F33 formula, the EE% is significantly lower, possibly due to the substantial increase in PS. Also, the EE% for F35 is very low (about 7%). This may be due to the high stirrer speed, which generates high motion and turbulence, expelling the drug from the resultant NPs and decreasing the EE%.

The EE% of the prepared NPs is relatively low, which can be attributed to the physicochemical properties of BTZ and its interaction with albumin. BTZ is generally a small, partially hydrophilic molecule with limited hydrophobic domains, making it difficult for BTZ to be incorporated into albumin foldings and binding pockets, which are usually hydrophobic. Drug incorporation into ANPs is generally mediated by weak non-covalent hydrogen bonding, which is insufficient to ensure strong retention and entrapment of the drug within the NPs, especially for hydrophilic molecules, which prefer partitioning into aqueous media. This result has been reported in previous studies on albumin-based nanoparticles carrying hydrophilic drugs, in which low EE% is recognized as a limiting factor for the formulation and manufacturing of these drugs as ANPs⁴².

Although the encapsulation efficiency (EE%) of BTZ–HSA nanoparticles was calculated to be relatively low (36%), it should be emphasized that this value primarily reflects the formulation process rather than the drug content of the final administered formulation. EE% is conventionally determined by comparing the amount of drug initially added to the amount remaining unencapsulated in the supernatant after nanoparticle formation and centrifugation. This metric is therefore useful for evaluating and comparing formulation performance among different preparation conditions. Importantly, however, the preparation protocol includes a separation step in which the nanoparticle pellet, containing the encapsulated BTZ, is isolated by centrifugation and subsequently redispersed in the original volume (5 mL) of distilled water, while the supernatant containing the non-entrapped drug is discarded. As a result, the final nanoparticle dispersion used for *in vitro* and *in vivo* experiments consists predominantly of BTZ-loaded nanoparticles with minimal free drug, effectively yielding a formulation with a high fraction of entrapped BTZ despite the moderate EE% calculated during process evaluation. Therefore, the reported EE% should be interpreted as an indicator of formulation efficiency rather than a direct measure of drug availability in the administered nanoparticle suspension.

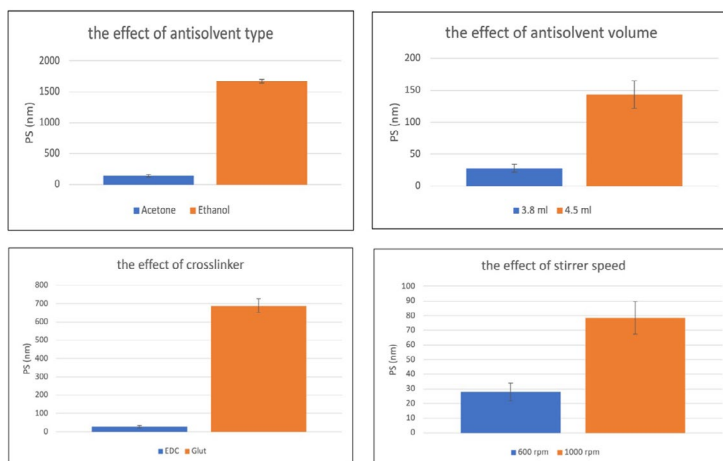


Figure 1. The effect of process parameters on PS, the results are presented as average \pm SD

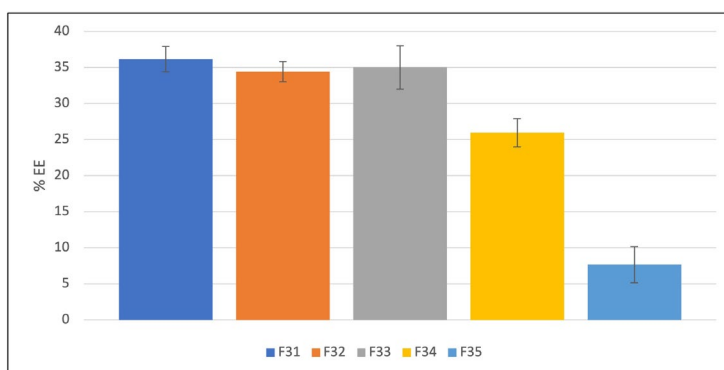


Figure 2. The EE% of the prepared NPs, the results are presented as average \pm SD

The optimized formula was selected based on the lowest PS and PDI, but the highest EE%. This formula is F31, which has 28.8 nm, 0.045, and 36% PS, PDI, and EE%, respectively. The PS distribution chart is shown in Figure 3.

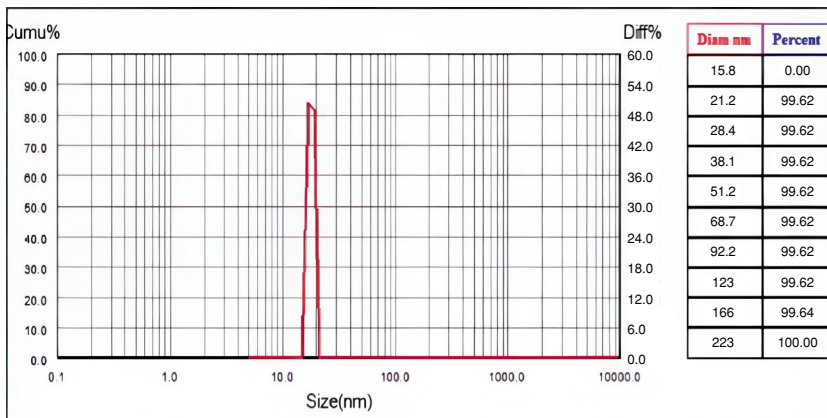


Figure 3. Particle size distribution of the optimized formula

Cumulative release of BTZ

Cumulative *in vitro* release of BTZ from BTZ HSA NP is shown in Figure 4. The release was performed at pH 5.5 to simulate the tumor microenvironment and at pH 7.4 to simulate the systemic circulation, and in both conditions, the BTZ HSA NPs dosage form exhibited a biphasic sustained-release profile. A significant initial burst (30% within the first hour) followed by a slower release reaching about 85% after 24 hs. In contrast, the pure drug showed an initial burst and fast dissolution (ca. 100% cumulative release within the first hour).

The *in vitro* release of BTZ from NPs was initially rapid, possibly due to desorption of drug bound to the surface or release from the outer superficial layer(s) of the matrix. Then, the release slowed to approximately 85% after 24 hours, indicating that a significant amount of BTZ was entrapped in or slowly diffused through the protein network over the test period. The burst and delayed second-phase release, combined, indicate that albumin nanoparticles significantly modify the release of BTZ relative to the free drug. This feature should enhance the pharmacokinetic half-life and minimise peak *in vivo*⁴³.

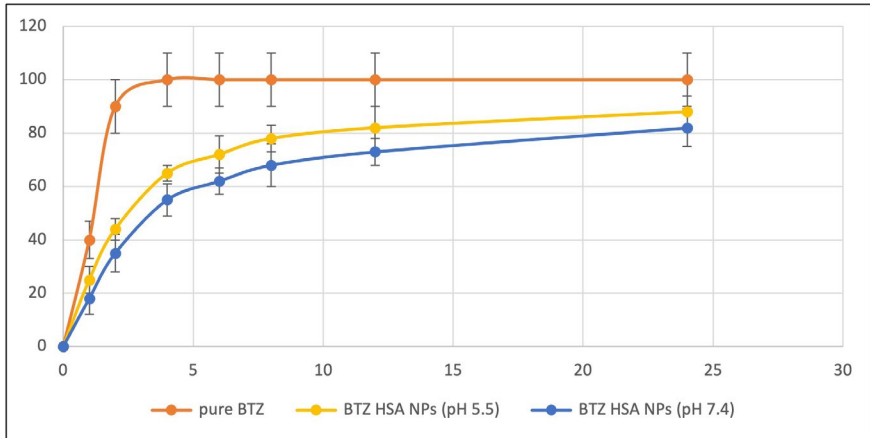


Figure 4. *In vitro* release of BTZ from pure BTZ and BTZ HSA NPs

Morphology of BTZ HSA NPs

The prepared NPs exhibit a near-spherical morphology with diameters less than 50 nm, as shown in Figure 5. These images are consistent with the results of light-scattering measurements. The images were obtained at two different magnifications, with a scale bar of 50 nm and 100 nm. Also, the images show minimal aggregation of the BTZ NPs.

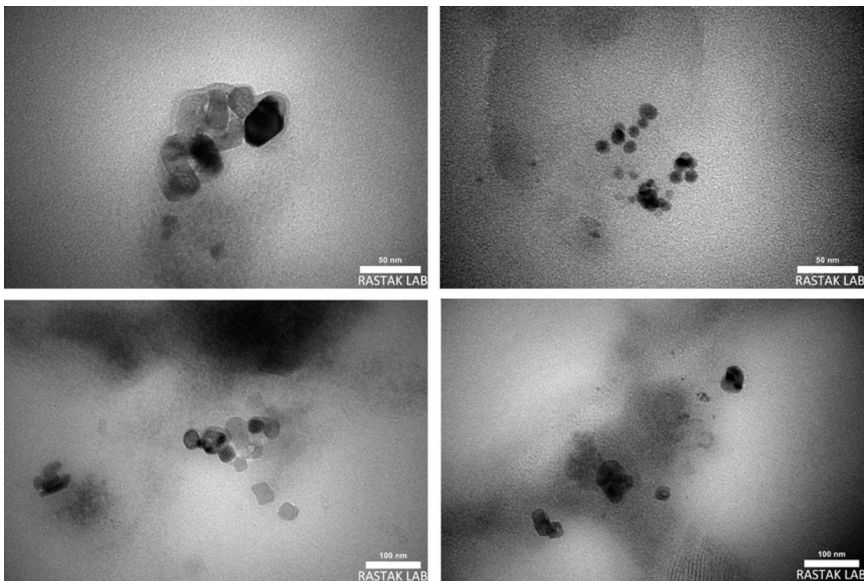


Figure 5. TEM images of BTZ HSA NPs

Hemolysis test

The results of the hemolysis test showed that the percentage of hemolysis was less than 2% with the highest concentration of BTZ HSA NPs, which is most commonly accepted as indicating that the NPs are biocompatible in the blood after administration and do not damage blood cells^{44,45}. The results for this test are illustrated in Table 2.

Table 2. The hemolysis test for BTZ HSA NPs

Samples	Concentration (mg/ml)	Absorbance at Wavelength 540 nm	Hemolysis %
1	20	0.094	1.55
2	10	0.09	1.36
3	5	0.078	0.82
4	2.5	0.074	0.64
5	1.25	0.069	0.41
6	0.625	0.064	0.18
7	0.313	0.063	0.14
8	0.156	0.061	0.05

In vitro cytotoxicity study

This study is performed based on the reduction of the yellow tetrazolium salt, MTT (3-(4,5-dimethylthiazol-2-yl)-2,5-diphenyltetrazolium bromide), to insoluble purple formazan crystals by mitochondrial dehydrogenase enzymes present only in metabolically active (viable) cells. This enzymatic reduction occurs predominantly in the mitochondria, and the amount of formazan produced is directly proportional to the number of viable cells in the sample⁴⁶.

The results for the *in vitro* cytotoxicity study are illustrated in Figure 6. The MTT assay showed that the blank NPs are non-toxic even at very high concentrations, up to 1000 ng/mL. On the other hand, the percentage of viable cells treated with BTZ HSA NPs has decreased compared with the cells treated with pure BTZ solution in a concentration range (0-5 ng/mL). After that, the cytotoxicity appears similar. IC₅₀ of pure BTZ solution is 2.07 nM, while for BTZ HSA NPs is 2.2 nM⁴⁷.

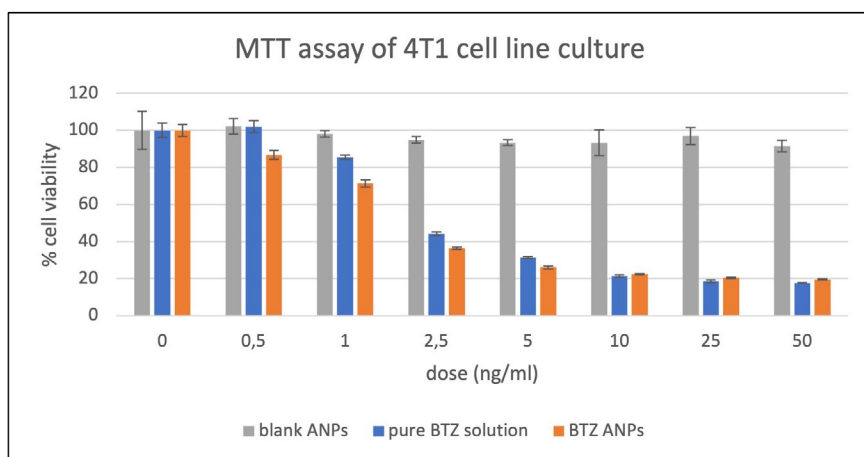


Figure 6. *In vitro* cytotoxicity of Blank ANPs, pure BTZ and BTZ HSA NPs

Antitumor activity

Tumor volume was measured for each mouse for 14 days, and the results are shown in Figure 7. The results are presented as the mean \pm SD. The group that received BTZ HSA NPs showed a significant difference ($p=0.0028$) compared with the group that received pure BTZ solution. Also, the group that received only PBS (Control) showed a significant increase in tumor volume over the treatment period.

Tumor volume was monitored over 14 days across three treatment groups: PBS, pure BTZ, and BTZ HSA NPs. Specifically, ***in vitro* cytotoxicity studies using the 4T1 cell line demonstrated that Blank HSA NPs were non-toxic and did not induce any cell killing**, indicating that the albumin carrier itself does not contribute to antitumor activity. Based on these results, and to avoid unnecessary animal suffering, we did not include an additional *in vivo* blank NP group. The PBS group showed a steady increase in tumor size, reaching nearly 400 mm³ by day 14, confirming the absence of therapeutic effect. Treatment with pure BTZ moderately slowed tumor growth, while BTZ HSA NPs demonstrated improved suppression. Notably, the BTZ HSA NPs group exhibited the most pronounced reduction in tumor volume, maintaining consistently low levels throughout the study. These results suggest that nanoparticle-based delivery of BTZ enhances its antitumor efficacy, likely due to improved bioavailability and targeted action^{48,49}.

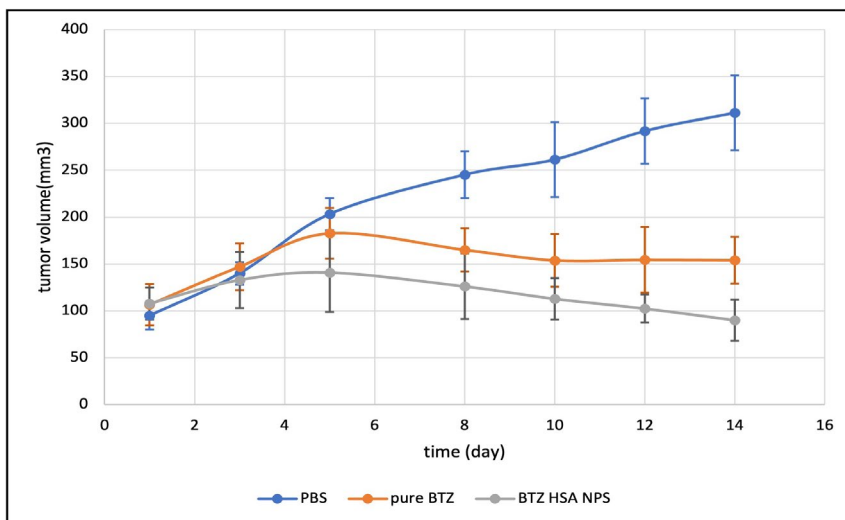


Figure 7. Tumor volume analysis of all three groups received three different treatments. The results are represented as average \pm SD.

Histopathology examination

The histopathological study results are illustrated in Table 3 and Figure 8.

After examining the histopathology slides, the interpretation was that the BTZ HSA NPs showed signs of effective treatment (treatment effects), decreased tumor aggressiveness (lower mitotic count and nuclear pleomorphism), increased apoptosis, and improved immune cell infiltration compared to Control and BTZ alone.

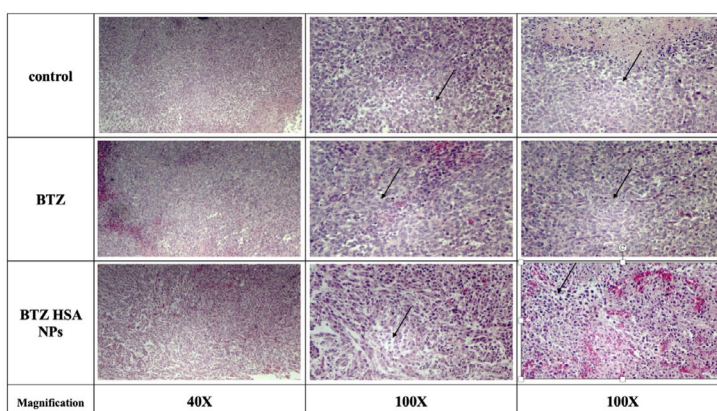


Figure 8. Histopathological examination of tumor tissue after treatment with PBS, BTZ, and BTZ HSA NPs

Table 3. Histopathological explanation for the tumor tissues after treatment with PBS, BTZ, and BTZ HSA NPs

Criteria	Groups		
	Control	BTZ	BTZ HSA NPs
Tumor necrosis	Less than 30-40% Moderate level of tumor necrosis, suggesting some degree of tumor aggressiveness, but not excessively high	Less than 30-40% Similar to Control: moderate necrosis	Less than 20-30% Lower necrosis compared to Control and BT2, possibly indicating less aggressive behaviour or better tumor viability
Mitotic count	31 High mitotic activity, indicating rapid tumor cell proliferation	29 Slightly lower than Control but still high, indicating rapid proliferation	18 Substantially lower mitotic activity, suggesting reduced tumor cell proliferation
Apoptotic figures count	6 Moderate apoptosis, showing some tumor cell death	7 Similar apoptosis level compared to the Control	10 Increased apoptosis, indicating more tumor cell death
Nuclear pleomorphism	+3 (high) Indicates a high grade of nuclear atypia, suggesting aggressive tumor behaviour with rapid growth	+3 (high) High nuclear atypia, like Control	+2 (moderate) A lower degree of nuclear atypia compared to the Control and BTZ, suggesting a reduced malignancy grade
Treatment effects	Not present No evidence that treatment is impacting the tumor	Not present No treatment impact visible	Present Indicating that the tumor shows histologic signs of treatment response
Tumor-Infiltrating Lymphocytes	Less than 1% Very low infiltration of inflammatory (immune) cells, which often correlates with poor antitumor immune response	Less than 1% Very low immune cell infiltration	Less than 4% Higher infiltration of inflammatory cells compared to Control and BTZ, which may be a positive prognostic factor reflecting immune engagement

Stability study

The stability study for the BTZ HSA NPs was conducted for 60 days at 4°C and 25°C. Each formula was evaluated based on its PS, PDI, and EE% every two weeks in this period. The results for this study are illustrated in Figures 9, 10, and 11.

The results showed that the prepared BTZ ANPs retain their PS and EE% when stored at 4°C, whereas PS and PDI increase substantially when stored at 25°C. On the other hand, the NPs stored at room temperature showed a significant decrease in the EE%. The increase in PS can be explained by the

higher temperature, which promotes particle motion, agglomeration, and particle growth. Also, increased motion may encourage drug leakage from the NPs, thereby decreasing the EE%.

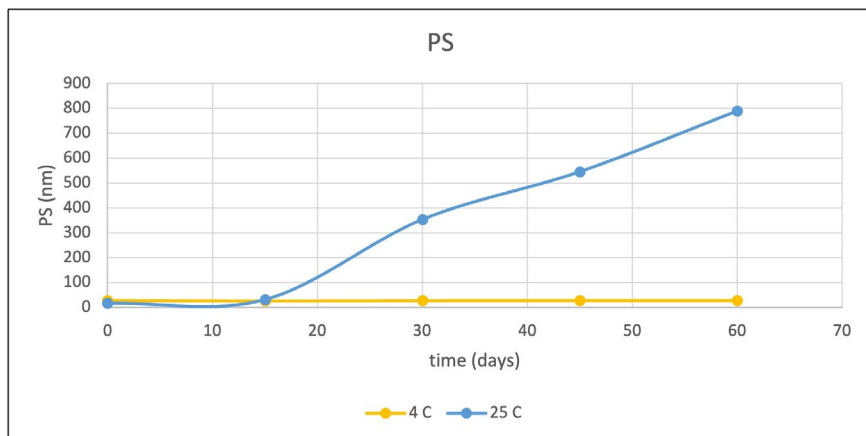


Figure 9. The PS change of BTZ HSA NPs over 60 days at 4°C and 25°C

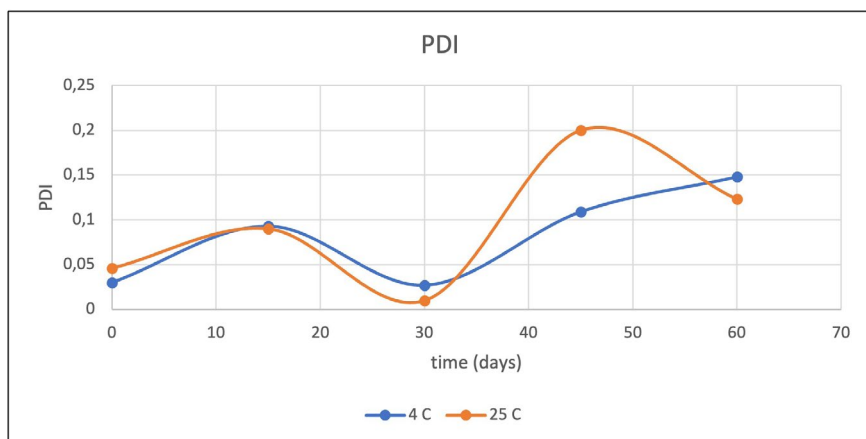


Figure 10. The PDI change of BTZ HSA NPs over 60 days at 4°C and 25°C

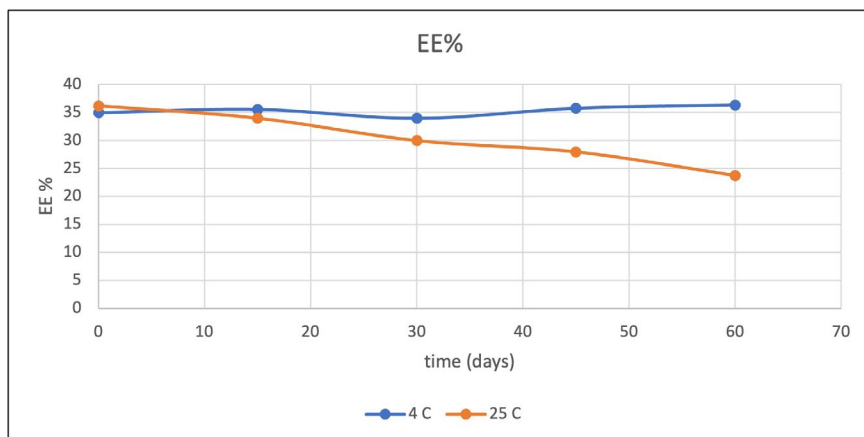


Figure 11. The EE% change of BTZ HSA NPs over 60 days at 4°C and 25°C

In conclusion, the formulation of BTZ as HSA nanoparticles represents a promising and effective strategy to enhance the therapeutic efficacy and selectivity of this potent anticancer drug. The desolvation method proved to be a simple, reliable, and reproducible technique for preparing nanoparticles with desirable physicochemical characteristics. *In vitro* release studies demonstrated a biphasic release profile characterised by an initial burst followed by a sustained release phase, suggesting efficient drug diffusion from the protein matrix and potential for prolonged therapeutic action. Moreover, the *in vivo* evaluation confirmed that nanoparticle encapsulation improved the pharmacokinetic profile and tumor-targeting potential of BTZ while reducing systemic toxicity, indicating enhanced therapeutic selectivity.

Overall, this study provides a solid foundation for developing protein-based nanocarriers for the delivery of anticancer drugs. The findings suggest that HSA nanoparticles are a promising biocompatible system capable of improving the therapeutic index of Bortezomib and potentially other chemotherapeutic agents.

STATEMENT OF ETHICS

Animal experiments were approved by the ethical committee of the University of Baghdad- College of Pharmacy Research Ethics Committee (Approval No. RECAUBCP13220240A13-2-2024).

CONFLICT OF INTEREST STATEMENT

The authors declare no conflict of interest.

AUTHOR CONTRIBUTIONS

AA contributed to the design, analysis, interpretation, drafting, and writing of the manuscript. MM contributed to the revision and proofreading of the manuscript (supervisor).

FUNDING SOURCES

This research did not receive any specific grant from funding agencies in the public, commercial, or not-for-profit sectors.

ACKNOWLEDGMENTS

The authors of this manuscript would like to express their deepest gratitude to the pharmaceutical department, College of Pharmacy, University of Baghdad, for providing the resources and instruction necessary to make this work possible. We would also like to thank the Pharmaceutical Department, College of Pharmacy, University of Kufa, for their support and guidance.

REFERENCES

1. Roccaro AM, Vacca A, Ribatti D. Bortezomib in the treatment of cancer. *Recent Pat Anticancer Drug Discov*, 2006;1(3):397–403. Doi: 10.2174/157489206778776925
2. Piperdi B, Ling Y-H, Liebes L, Muggia F, Perez-Soler R. Bortezomib: understanding the mechanism of action. *Mol Cancer Ther*, 2011;10(11):2029–2030. Doi: 10.1158/1535-7163.mct-11-0745
3. Liu J, Zhao R, Jiang X, Li Z, Zhang B. Progress on the application of bortezomib and bortezomib-based nanoformulations. *Biomolecules*, 2021;12(1):51. Doi: 10.3390/biom12010051
4. Voorhees PM, Orlowski RZ. The proteasome and proteasome inhibitors in cancer therapy. *Annu Rev Pharmacol Toxicol*, 2006;46:189–213. Doi: 10.1146/annurev.pharmtox.46.120604.141300
5. Jaracz S, Chen J, Kuznetsova LV, Ojima I. Recent advances in tumor-targeting anticancer drug conjugates. *Bioorg Med Chem*, 2005;13(17):5043–5054. Doi: 10.1016/j.bmc.2005.04.084
6. Zuccari G, Milelli A, Pastorino F, Loi M, Petretto A, Parise A, et al. Tumor vascular targeted liposomal-bortezomib minimizes side effects and increases therapeutic activity in human neuroblastoma. *JCR*, 2015;211:44–52. Doi: 10.1016/j.jconrel.2015.05.286
7. Liu S, Ono RJ, Yang C, Gao S, Ming Tan JY, Hedrick JL, et al. Dual pH-responsive shell-cleavable polycarbonate micellar nanoparticles for *in vivo* anticancer drug delivery. *ACS Appl Mater Interfaces*, 2018;10(23):19355–19364. Do: 10.1021/acsami.8b01954
8. Liu L, Wang S, Qi P, Song S, Yang Y, Shi J, Han G. Dopamine-modified poly (ϵ -caprolactone) micelles for pH controlled delivery of bortezomib. *Int J Pharm*, 2020;590:119885. Doi: 10.1016/j.ijpharm.2020.119885
9. Xu B, Li S, Shi R, Liu H. Multifunctional mesoporous silica nanoparticles for biomedical applications. *Signal Transduct Target Ther*, 2023;8(1):435. Doi: 10.1038/s41392-023-01654-7
10. Vysyaraju NR, Paul M, Ch S, Ghosh B, Biswas S. Olaparib@human serum albumin nanoparticles as sustained drug-releasing tumor-targeting nanomedicine to inhibit growth and metastasis in the mouse model of triple-negative breast cancer. *J Drug Target*, 2022;30(10):1088–1105. Doi: 10.1080/1061186X.2022.2092623
11. Kratz F. Albumin as a drug carrier: design of prodrugs, drug conjugates and nanoparticles. *JCR*, 2008;132(3):171–183. Doi: 10.1016/j.jconrel.2008.05.010
12. Hoogenboezem EN, Duvall CL. Harnessing albumin as a carrier for cancer therapies. *Adv Drug Deliv Rev*, 2018;130:73–89. Doi: 10.1016/j.addr.2018.07.011
13. Sulowska A, Równicka J, Bojko B, Sulowski W. Interaction of anticancer drugs with human and bovine serum albumin. *J Mol Struct*, 2003;651:133–140. Doi: 10.1016/S0022-2860(02)00642-7
14. Weber C, Coester C, Kreuter J, Langer K. Desolvation process and surface characterisation of protein nanoparticles. *Int J Pharm*, 2000;194(1):91–102. Doi: 10.1016/S0378-5173(99)00370-1
15. Jahanban-Esfahlan A, Dastmalchi S, Davaran S. A simple improved desolvation method for the rapid preparation of albumin nanoparticles. *Int J Biol Macromol*, 2016;91:703–709. Doi: 10.1016/j.ijbiomac.2016.05.032
16. Langer K, Balthasar S, Vogel V, Dinauer N, von Briesen H, Schubert D. Optimization of the preparation process for human serum albumin (HSA) nanoparticles. *Int J Pharm*. 2003;257(1-2):169–180. Doi: 10.1016/s0378-5173(03)00134-0
17. Eglä M, Rajab NA. Sericin-based paclitaxel nanoparticles: preparation and physicochemical evaluation. *Iraqi J Pharm Sci*, 2024; 33(4SI):169–178. Doi: 10.31351/vol33iss(4SI)pp169-178

18. Wais FMH, Alhagiesia AW, Oudah MH. Preparation and evaluation of ibuprofen nanosuspension for solubility enhancement. *Gomal J Med Sci*, 2025;23:127–131. Doi: 10.46903/gjms/23.1.Special.1763
19. Al-Edresi S, Abdul-Hasan MT, Hadi Salal YA. Formulation, analysis and validation of nanosuspensions-loaded voriconazole to enhance solubility. *Int J Appl Pharm*, 2024;16(2):209–214. Doi: 10.22159/ijap.2024v16i2.49591
20. Sulaiman HT, Rajab NA. Olmesartan medoxomil nanomicelle using Soluplus for dissolution enhancement: preparation, *in-vitro* and *ex-vivo* evaluation. *Iraqi J Pharm Sci*, 2025;34(2):47–59. Doi: 10.31351/vol34iss2pp47-59
21. Alwan ZS, Rajab NA. Preparation and characterization of febuxostat as nanosuspension. *Iraqi J Pharm Sci*, 2024;33(4SI):261–270. Doi: 10.31351/vol33iss(4SI)pp261-270
22. Luis de Redín I, Boiero C, Martínez-Ohárriz MC, Agüeros M, Ramos R, Peñuelas I, et al. Human serum albumin nanoparticles for ocular delivery of bevacizumab. *Int J Pharm*, 2018;541(1-2):214–223. Doi: 10.1016/j.ijpharm.2018.02.003
23. Ramadhan SH, Al-Kinani KK. Statistical optimization and characterization of nimodipine transferosomes. *Al-Rafidain J Med Sci*, 2024;7(1S):77–83. Doi: 10.54133/ajms.v7i1(Special).1015
24. Zhang J, Fu X, Yan C, Wang G. The morphology dependent interaction between silver nanoparticles and bovine serum albumin. *Materials*, 2023;16(17):5821. Doi: 10.3390/ma16175821
25. Kudłacik-Kramarczyk S, Drabczyk A, Głab M, Gajda P, Czopek A, Zagórska A, et al. The development of the innovative synthesis methodology of albumin nanoparticles supported by their physicochemical, cytotoxic and hemolytic evaluation. *Materials*, 2021;14(16):4386. Doi: 10.3390/ma14164386
26. Hasan HJ, Ghareeb MM. Optimizing desolvation conditions for glutathione-cross-linked bovine serum albumin nanoparticles: implication for intravenous drug delivery. *Cureus*, 2024;16(9):e69514. Doi: 10.7759/cureus.69514
27. Wan X, Zheng X, Pang X, Zhang Z, Jing T, Xu W, et al. The potential use of lapatinib-loaded human serum albumin nanoparticles in the treatment of triple-negative breast cancer. *Int J Pharm*, 2015;484(1-2):16–28. Doi: 10.1016/j.ijpharm.2015.02.037
28. Kim TH, Jiang HH, Youn YS, Park CW, Tak KK, Lee S, et al. Preparation and characterization of water-soluble albumin-bound curcumin nanoparticles with improved antitumor activity. *Int J Pharm*, 2011;403(1-2):285–291. Doi: 10.1016/j.ijpharm.2010.10.041
29. Zhang H, Dong S, Zhang S, Li Y, Li J, Dai Y, et al. pH-responsive lipid polymer hybrid nanoparticles (LPHNs) based on poly (β -amino ester) as a promising candidate to resist breast cancers. *J Drug Deliv Sci Technol*, 2021;61:102102. Doi: 10.1016/j.jddst.2020.102102
30. See SHC, Siziopikou KP. Pathologic evaluation of specimens after neoadjuvant chemotherapy in breast cancer: current recommendations and challenges. *Pathol Res Pract*, 2022;230:153753. Doi: 10.1016/j.prp.2021.153753
31. Kim D, Lee SS, Yoo WY, Moon H, Cho A, Park SY, et al. Combination therapy with doxorubicin-loaded reduced albumin nanoparticles and focused ultrasound in mouse breast cancer xenografts. *Pharmaceuticals (Basel)*, 2020;13(9):235. Doi: 10.3390/ph13090235
32. Alkufi HK, Kassab HJ. Soluplus-stabilized nimodipine-entrapped spanlastic formulations prepared with edge activator (Tween20): comparative physicochemical evaluation. *Pharm Nanotechnol*, 2024;13(3):551–563. Doi: 10.2174/0122117385348551241028102256
33. Al-Shammari AH, Ali Shahadha MA. The effect of Favipiravir on liver enzyme among patients with mild to moderate COVID-19 infection: a prospective cohort study. *J Popul Ther Clin Pharmacol*, 2022;29(4):e46–e54. Doi: 10.47750/jptcp.2022.967

34. Manna MJ, Baqir LS, Abdulmir HA. The assessment of the antimicrobial effect of gemfibrozil alone or in combination with ceftriaxone or gentamycin on several types of bacteria. *Acta Pharm Sci*, 2024;62(3):565–574. Doi: 10.23893/1307-2080.APS6235
35. Al-Mahmood S, Rajab NA. Effect of unsaturated fatty acids on the topical delivery of caspofungin ufasomes: *in vitro*/ *ex vivo* evaluation and anti-fungal study against *Candida albicans*. *OpenNano*, 2025;24:100250. Doi: 10.1016/j.onano.2025.100250
36. Mohammad-Beigi H, Shojaosadati SA, Morshedi D, Mirzazadeh N, Arpanaei A. The effects of organic solvents on the physicochemical properties of human serum albumin nanoparticles. *Iran J Biotechnol*, 2016;14(1):45–50. Doi: 10.15171/ijb.1168
37. Taheri ES, Jahanshahi M, Mosavian MTH. Preparation, characterization and optimization of egg albumin nanoparticles as low molecular-weight drug delivery vehicle. *Part Part Syst Charact*, 2012;29(3):211–222. Doi: 10.1002/ppsc.201100037
38. von Storp B, Engel A, Boeker A, Ploeger M, Langer K. Albumin nanoparticles with predictable size by desolvation procedure. *J Microencapsul*, 2012;29(2):138–146. Doi: 10.3109/02652048.2011.635218
39. Kadhum RW, Abd-Alhammid SN. Process factors affecting the preparation and characterization of dutasteride nanosuspension. *Iraqi J Pharm Sci*, 2025;34(1):35–48. Doi: 10.31351/vol34iss1pp35-48
40. Prajapati R, Garcia-Garrido E, Somoza Á. Albumin-based nanoparticles for the delivery of Doxorubicin in breast cancer. *Cancers (Basel)*, 2021;13(12):3011. Doi: 10.3390/cancers13123011
41. Alhagiesha AW, Ghareeb MM. Formulation and evaluation of nimodipine nanoparticles incorporated within orodispersible tablets. *Int J Drug Deliv Technol*, 2020;10(4):547–552. Doi: 10.25258/ijddt.10.4.7
42. Tambuwala MM, Khan MN, Thompson P, McCarron PA. Albumin nano-encapsulation of caffeic acid phenethyl ester and piceatannol potentiated its ability to modulate HIF and NF- κ B pathways and improves therapeutic outcome in experimental colitis. *Drug Deliv Transl Res*, 2019;9(1):14–24. Doi: 10.1007/s13346-018-00597-9
43. Elzoghby AO, Samy WM, Elgindy NA. Albumin-based nanoparticles as potential controlled release drug delivery systems. *J Control Release*, 2012;157(2):168–182. Doi: 10.1016/j.jconrel.2011.07.031
44. Qu N, Lee RJ, Sun Y, Cai G, Wang J, Wang M, et al. Cabazitaxel-loaded human serum albumin nanoparticles as a therapeutic agent against prostate cancer. *Int J Nanomedicine*, 2016;11:34519. Doi: 10.2147/IJN.S105420
45. Nosrati H, Rakhshbahar A, Salehiabar M, Afroogh S, Kheiri Manjili H, Danafar H, et al. Bovine serum albumin: an efficient biomacromolecule nanocarrier for improving the therapeutic efficacy of chrysin. *J Mol Liq*, 2018;271:639–646. Doi: 10.1016/j.molliq.2018.06.066
46. Chhabria D, Sundaram GA, Ganapathy D, Balasubramanian P. Unveiling the biomedical and photocatalytic properties of copper(II) imidazole complex-functionalized TiO₂ nanoparticles. *J Mol Liq*, 2025;426. Doi: 10.1016/j.molliq.2025.127368
47. Lohberger B, Steinecker-Frohnwieser B, Stuendl N, Kaltenegger H, Leithner A, Rinner B. The proteasome inhibitor bortezomib affects chondrosarcoma cells via the mitochondria-caspase dependent pathway and enhances death receptor expression and autophagy. *PLoS One*, 2016;11(12):e0168193. Doi: 10.1371/journal.pone.0168193
48. Fu Q, Sun J, Zhang W, Sui X, Yan Z, He Z. Nanoparticle albumin-bound (NAB) technology is a promising method for anti-cancer drug delivery. *Recent Pat Anticancer Drug Discov*, 2009;4(3):262–272. Doi: 10.2174/157489209789206869
49. Dawoud MHS, Abdel-Daim A, Nour MS, Sweed NM. A quality by design paradigm for albumin-based nanoparticles: formulation optimization and enhancement of the antitumor activity. *J Pharm Innov*, 2023;18(3):1395–1414. Doi: 10.1007/s12247-022-09698-y